

The cycle is therefore partly decoupled from the oxidation of organic matter or the reduction of electron acceptors.

The thiosulfate shunt can help account for the large isotopic fractionation of  $^{34}\text{S}$  to  $^{32}\text{S}$  between sulfate and sulfides in sediments. It has long been an enigma why the apparent isotopic fractionation during sulfate reduction in marine sediments is commonly between 35 and 60 per mil whereas pure cultures of sulfate reducing bacteria cause a fractionation of only 10 to 30 per mil (15). Recycling via thiosulfate will tend to increase the isotopic difference between sulfate and reduced S, mostly because the inner (+6) S atom of thiosulfate is strongly enriched in  $^{34}\text{S}$  relative to the outer (-2) S atom (16). When the  $\text{S}_2\text{O}_3^{2-}$  is disproportionated, the  $^{34}\text{S}$ -rich inner atoms are converted to  $\text{SO}_4^{2-}$  while the  $^{34}\text{S}$ -poor outer atoms are converted to  $\text{HS}^-$ . The thiosulfate shunt will thereby tend to recycle lighter S in the reduced state and convert heavier S to sulfate.

#### REFERENCES AND NOTES

1. B. B. Jørgensen, *Nature* **296**, 643 (1982); P. M. Crill and C. S. Martens, *Geochim. Cosmochim. Acta* **51**, 1175 (1987); J. P. Christensen, *Cont. Shelf Res.* **9**, 223 (1989).
2. B. B. Jørgensen, M. Bang, T. H. Blackburn, *Mar. Ecol. Prog. Ser.* **59**, 39 (1990).
3. R. W. Howarth, *Biogeochemistry* **1**, 5 (1984); R. C. Aller and P. D. Rude, *Geochim. Cosmochim. Acta* **52**, 751 (1988).
4. Yu. I. Sorokin, *J. Cons. Cons. Int. Explor. Mer.* **34**, 423 (1972); F. J. Millero, *Mar. Chem.* **18**, 121 (1986); C. O. Moses, D. K. Nordstrom, J. S. Herman, A. L. Mills, *Geochim. Cosmochim. Acta* **51**, 1561 (1987).
5. F. Bak and H. Cypionka, *Nature* **326**, 891 (1987).
6. F. Bak and N. Pfennig, *Arch. Microbiol.* **147**, 184 (1987).
7. H. Fossing and B. B. Jørgensen, in preparation.
8. B. B. Jørgensen, unpublished data.
9. — and F. Bak, unpublished data.
10. M. Krämer and H. Cypionka, *Arch. Microbiol.* **151**, 232 (1989).
11. F. Bak, thesis, University of Konstanz, GFR (1988).
12. F. Widdel, in *Biology of Anaerobic Microorganisms*, A. J. B. Zehnder, Ed. (Wiley, New York, 1988), pp. 469–585.
13. D. P. Kelly, in *Autotrophic Bacteria*, H. G. Schlegel and B. Bowien, Eds. (Science Tech, Madison, 1989), pp. 193–218.
14. G. W. Luther III et al., *Science* **232**, 746 (1986).
15. L. A. Chambers and P. A. Trudinger, *Geomicrobiol. J.* **1**, 249 (1979).
16. F. Uyama, H. Chiba, M. Kusakabe, H. Sakai, *Geochem. J.* **19**, 301 (1985).
17. Results are from a single but representative slurry experiment. The isotopes were added to two separate but identical slurries kept under  $\text{N}_2$  at 22°C. The sandy mud had an organic content of 1.8% dry weight. In situ temperature was 4°C and salinity was 15 per mil. The in situ  $\text{SO}_4^{2-}$  concentration was 13 mM, and  $\text{S}_2\text{O}_3^{2-}$  was below the detection limit by ion chromatography, 10  $\mu\text{M}$ . An unlabeled pool, 75  $\mu\text{M}$ , of  $\text{S}_2\text{O}_3^{2-}$  was therefore added to the two identical slurries. The sediment contained 81  $\mu\text{M}$   $\text{HS}^-$  plus 8.2  $\mu\text{mol}$  of  $\text{FeS}$  and 19.9  $\mu\text{mol}$  of  $\text{FeS}_2$  per gram of slurry. Subsamples were taken without air contact, fixed with  $\text{ZnCl}_2$ , and centrifuged. Radiolabeled  $\text{S}_2\text{O}_3^{2-}$  and  $\text{SO}_4^{2-}$  were separated in the supernatant by ion chromatography and counted. Reduced  $^{35}\text{S}$  ( $\text{S}_{\text{red}}$ ) comprised  $\text{HS}^-$ ,  $\text{S}_7^{2-}$ ,  $\text{S}^0$ ,  $\text{FeS}$ , and  $\text{FeS}_2$  and was all collected by  $\text{H}_2^{35}\text{S}$  distillation

from washed sediment by the chromium reduction technique (18) and counted. Radioactivities are expressed as percent of added  $^{35}\text{S}_2\text{O}_3^{2-}$  radioactivity.

18. N. N. Zhabina and I. I. Volkov, in *Environmental Biogeochemistry and Geomicrobiology*, W. E. Krumbain, Ed. (Ann Arbor Science, Ann Arbor, MI, 1978), vol. 3, pp. 735–746; J. T. Westrich, thesis, Yale University, New Haven (1983).
19. Sediment cores were incubated for 18 hours at the in situ temperature (5.5°C). The sediment was sandy mud from 33-m water depth; organic content was 4% dry weight. The  $^{35}\text{S}$ -tracer techniques are de-

scribed in (7, 20).

20. H. Fossing and B. B. Jørgensen, *Biogeochemistry* **8**, 205 (1989).
21. I thank D. T. Thomsen for technical assistance and F. Bak and H. Fossing for inspiring discussions. I am grateful to B. Kruse for an invitation to join a cruise on RV *Gunnar Thorson* in Kattegat. Financial support was given by the Danish Ministry of the Environment and the Danish Natural Science Research Council.

23 February 1990; accepted 2 May 1990

## Hind Limbs of Eocene *Basilosaurus*: Evidence of Feet in Whales

PHILIP D. GINGERICH, B. HOLLY SMITH, ELWYN L. SIMONS

New specimens of middle Eocene *Basilosaurus isis* from Egypt include the first functional pelvic limb and foot bones known in Cetacea. These are important in corroborating the intermediate evolutionary position of archaeocetes between generalized Paleocene land mammals that used hind limbs in locomotion and Oligocene-to-Recent whales that lack functional pelvic limbs. The foot is paraxonic, consistent with derivation from mesonychid Condylarthra. Hind limbs of *Basilosaurus* are interpreted as copulatory guides.

WHALES ARE REMARKABLE among mammals in being fully aquatic, and their transition from land to sea is among the most interesting problems of evolution (1–3). Most mammals use limbs, particularly hind limbs, in locomotion. Modern cetaceans live in water and lack hind limbs entirely, retaining only rod-like vestiges of pelvic bones, femora, and rarely tibiae embedded in musculature of the ventral body wall (4, 5). Limbs are important for understanding the early evolution of whales. Hind limb buds have long been known in embryonic cetaceans up to 32-mm crown-rump length (6), and adults with externally projecting rudiments are also known (7). We now describe evidence of functional hind limbs in a cetacean.

*Basilosaurus* is a large serpentine Eocene vertebrate discovered early in the 19th century when it was described as a reptile and named “king lizard” (8). Richard Owen demonstrated the mammalian characteristics of *Basilosaurus* and, within mammals, its cetacean affinities (9). Two species are known: *B. cetoides* from the late Eocene of the southeastern United States and *B. isis* from the late middle Eocene of Egypt (10, 11). The most complete *Basilosaurus* specimens known previously were two partial

skeletons of *B. cetoides* collected by C. Schuchert in Alabama in 1894 and 1896 for the U.S. National Museum (USNM). One of these specimens, USNM 12261, includes left and right innominate bones of the pelvis and a partial femur (12, 13); these remains were considered vestigial and functionless (14), an interpretation consistent with loss of functional hind limbs in modern whales.

In 1987 and 1989 we mapped 243 partial skeletons of *B. isis* and 77 partial skeletons of smaller archaeocetes (15) in the desert of Zeuglodon Valley (ZV), 50 km west of Fayum oasis in north central Egypt (16). All occur in a 90-m-thick stratigraphic section of shallow marine sandstones and shales of the Gehannam and Birket Qarun formations of late middle Eocene age (17). Excavations in 1989 yielded several nearly complete skeletons combined in the reconstruction shown in Fig. 1A. These indicate that *B. isis* had 7 cervical, 18 thoracic, and 42 lumbar and caudal vertebrae (Fig. 2), 9 more than the number of vertebrae shown in reconstructions of *B. cetoides* (13, 14). Limb and foot bones described here were all found in direct association with articulated skeletons of *B. isis* and undoubtedly represent this species. Specimens are conserved in the Cairo Geological Museum (CGM) and University of Michigan Museum of Paleontology (UM).

The innominate (Fig. 1B) is a straplike coossification of an elongated pubis and a relatively small ilium and ischium, each contributing to a well-defined acetabulum. The pubis and ischium surround a small obturator foramen. Left and right pubes fit together

P. D. Gingerich, Museum of Paleontology, University of Michigan, Ann Arbor, MI 48109–1079.

B. H. Smith, Museum of Anthropology, University of Michigan, Ann Arbor, MI 48109–1079.

E. L. Simons, Duke University Primate Center and Department of Anatomy and Anthropology, 3706 Erwin Road, Durham, NC 27705.

er at a robust unfused midline symphysis (18). The femur has a curved cylindrical head, a broad and high greater trochanter, considerable midshaft torsion, two flat facets for the patella, and distinct posteriorly directed medial and lateral condyles. The patella is relatively large, with a single flat femoral facet. The tibia and fibula are each only about one-half the length of the femur and are coossified at each end (Fig. 1B).

Tarsal bones exhibit a variable pattern of fusion at articulations that were probably immobile in life. Specimen UM 93231 has the astragalus, calcaneum, cuboid, and navicular coossified as one rigid bone (Fig. 1B), whereas CGM 42176 has the astragalus, navicular, ectocuneiform, and mesocuneiform fused (Fig. 3). Each specimen has a cuneiform articulating with the navicular and cuboid in the normal ectocuneiform position. A second cuneiform is much smaller and fused to the ectocuneiform as a mesocuneiform.

*Basilosaurus* lacks pedal digit I (hallux) entirely, and a beadlike mesocuneiform is the only remnant of digit II. Three metatarsals are known: one articulates with the distal surface of the ectocuneiform, identifying it as metatarsal III, and two articulate directly with the cuboid, identifying them as metatarsals IV and V. Metatarsal V is reduced relative to III and IV. The distal end of metatarsal III has a smooth flat surface for a proximal phalanx. The distal ends of metatarsals IV and V have more spherical surfaces for their proximal phalanges, suggesting a wider range of motion at these joints. Only one proximal phalanx is known. This fits onto metatarsal IV and has a small terminal second phalanx fused to it.

Metatarsals III and IV are the largest and longest metatarsals, making the foot paraxonic. A paraxonic pes in Cetacea is consistent with serological evidence of relationship to Artiodactyla (21) and dental evidence of derivation from mesonychid Condylarthra (22). Artiodactyla and mesonychid Condylarthra both have a paraxonic pes (23).

The inferred posture and range of motion of the hind limb of *Basilosaurus* are unusual for a mammal. On each side the innominate lay in the ventral body wall with the acetabulum opening downward. The femur has two distinct patellar surfaces lying at right angles to each other, one on the distal end and the other on the anterior surface. These surfaces are flat, and indicate two distinct stable positions of the patella relative to the femur. The two surfaces join along a convex narrowly rounded edge, indicating that a transition between stable positions of the patella was possible but that intermediate positions were unstable.

Articular surfaces on the femoral condyles

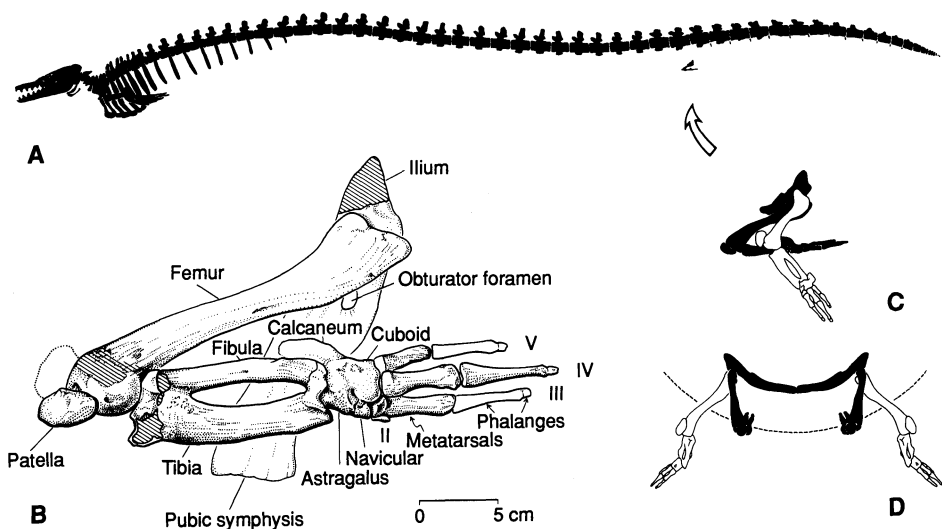


**Fig. 1.** Skeleton and hind limb of *B. isis* from the Birket Qarun Formation of Zeuglodon Valley, Egypt. (A) Skeleton in left lateral view showing body proportions and position of hind limb (arrow). Silhouette modified from Gidley (13) to reflect total of 67 vertebrae in *B. isis* and a total length of 16 meters. Serpentine body form suggests anguilliform locomotion, possibly in a shallow mangrove or seagrass habitat (for which there is some independent faunal evidence). (B) Left hind limb in normal resting posture, left ventrolateral view. Note the broad greater trochanter of femur, large patella, fusion of tibia and fibula, broad articulation of fibula and calcaneum, large projecting tuber of calcaneum, fusion of astragalus-calcaneum-cuboid-navicular, fusion of ectocuneiform-metatarsal III (and beadlike mesocuneiform remnant of pedal digit II), loss of pedal digit I (hallux) and great reduction of digit II, and reduction of distal phalanges on digit IV (phalanges of digits III and V are not yet known). Dotted outline shows alternate anterior position of patella. This reconstruction is a composite based on CGM 42176 (ZV-154), with fused tarsals and other foot bones from UM 93231 (ZV-132; also ZV-30). (C and D) Pelvic girdle and hind limb in resting posture (solid drawing) and functional extension (open outline), lateral and anterior views. Dashed line in anterior view shows approximate position of ventral body wall. Drawings in (B), (C), and (D) are based on an articulated full-sized model, but limb elements come from several specimens, making it difficult to measure excursion angles accurately.

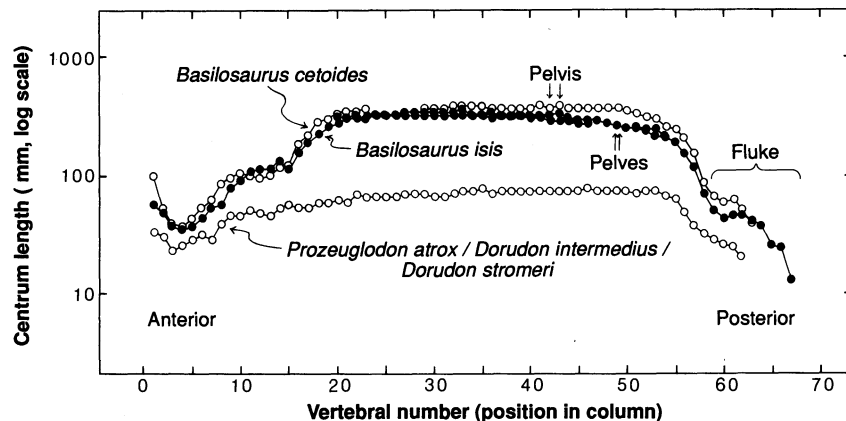


**Fig. 2.** Length-of-vertebrae profiles for three species of middle and late Eocene Archaeoceti. Lower profile (open circles) is based on a single specimen from Zeuglodon Valley in Egypt (ZV-1 in CGM), a dorudontine identified as *Prozeuglodon atrox*, *Dorudon intermedius*, or *D. stromeri* from the size of its skull and teeth; less complete specimens of *Zygorhiza kochii* from North America have similar profiles. Middle profile of Egyptian *B. isis* (closed circles) is based on three specimens from Zeuglodon Valley (ZV-30 with vertebrae numbered from 1 to 46, ZV-150 with vertebrae from 15 to 49, and ZV-148 with vertebrae from 46 to 67). Pelves were found near vertebra 49 in both CGM 42176 (ZV-154) and in ZV-167. Vertebral numbers are minima consistent with successive least-squares fits of vertebral lengths beginning with ZV-30. Upper profile of North American *B. cetoides* (open circles) is based on USNM 4675 and USNM 12261 from Alabama. Innominate of pelvis were found 22 and 21 vertebrae from end (12), near vertebrae numbered 42 and 43 here. *Basilosaurus isis* is smaller than *B. cetoides*, but their vertebral-length profiles are so similar that both probably represent the same genus (note rapid lengthening of posterior thoracic centra, beginning with vertebra 16, which is found only in *Basilosaurus*). True position of pelvis is probably between vertebrae 43 and 49 (shown between 45 and 46 in Fig. 1A, where the femur was found in ZV-30). Note sigmoid pattern at the posterior end of all three profiles. This pattern is present in the fluked tails of modern cetaceans, suggesting that *Basilosaurus* and other archaeocetes also had tails with flukes.

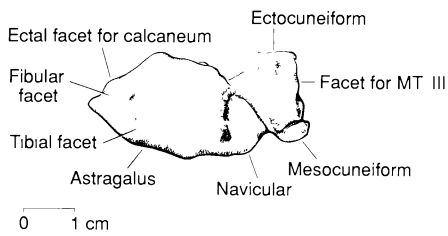


**Fig. 3.** Fused left astragalus, navicular, ectocuneiform, and mesocuneiform of *B. isis*, CGM 42176 (ZV-154), in ventrolateral view (see Fig. 1B for orientation). Note that fusion in this specimen includes the ectocuneiform and the mesocuneiform remnant of pedal digit II, but not the calcaneum or cuboid. MT, metatarsal.

are directed posteriorly, indicating that the knee was always flexed to some degree. The astragalus articulates with both the tibia and fibula, but the entire tibial facet is on the medial side of the astragalus, meaning that the foot was always supinated. The posterior position of the fibular trochlea formed by the astragalus and calcaneum indicates that the ankle was normally extended. Fitting articular surfaces together, with the patella positioned on the distal articular facet of the femur, yields a posture in which the femur points almost directly forward, and the rest of the limb extends backward from the knee (Fig. 1B, solid drawings in Fig. 1, C and D). This is interpreted as the habitual resting posture of the hind limb. Hydrodynamic considerations dictate that the femur was almost entirely within the body wall, while distal elements lay flat against the body wall externally.

The cylindrical shape of the femoral head indicates limited motion at the hip joint, with the femur rotating downward and outward from its resting position. A distinct apex of the patella extends beyond its articular surface on one side only (interpreted as proximal). Patellar asymmetry and the narrowly rounded edge separating patellar surfaces on the femur suggest a stabilizing mechanism locking the knee in partial extension when the patella was pulled onto the anterior surface of the femur. This unusual knee of *Basilosaurus* indicates a single alternative to its posture at rest. A downwardly rotated femur, extended locked knee, abducted hip, and dorsiflexed ankle are shown in open outline in Fig. 1, C and D.

Hind limbs of *Basilosaurus* appear to have been too small relative to body size (Fig. 1A) to have assisted in swimming, and they could not possibly have supported the body on land. However, maintenance of some function is likely for several reasons: most bones are present; some elements are fused, but remaining joints are well formed with little suggestion of degeneracy; the patella and calcaneal tuber are large for insertion of

powerful muscles; and the knee has a complex locking mechanism. The pelvis in generalized mammals supports reproductive organs in addition to its common use in locomotion. The pelvis of modern whales serves to anchor reproductive organs (5), even though functional hind limbs are lacking. Thus hind limbs of *Basilosaurus* are most plausibly interpreted as accessories facilitating reproduction. Abduction of the femur and plantar flexion of the foot, with the knee locked in extension, probably enabled hind limbs to be used as guides during copulation, which may otherwise have been difficult in a serpentine aquatic mammal.

Characteristics related to reproduction are often dimorphic in mammals, and dimorphism in a larger sample of limb elements would support the interpretation of hind limb function proposed here (lack of dimorphism would not necessarily refute it). Discovery of pelvic limbs and feet in *Basilosaurus* raises the possibility that other archaeocetes retained functional hind limbs (24). New specimens are required to test both hypotheses. In the meantime, retention of well-formed pelvic limbs in *Basilosaurus* corroborates the morphological primitiveness of archaeocetes. Temporal and morphological intermediates are direct and important evidence of transition in evolution: an Eocene whale with functional hind limbs narrows the gap considerably between generalized Paleocene land mammals that used hind limbs in locomotion and Oligocene-Recent modern whales that lack pelvic limbs.

#### REFERENCES AND NOTES

1. The oldest fossil whales are late early Eocene in age. *Pakicetus* and its relatives have teeth like later whales, but their auditory bullae are only partially modified for hearing in water and they are found in continental sediments with land mammals, suggesting that the transition had only begun (2). Nothing is known of the postcranial skeleton of *Pakicetus*. Middle and late Eocene whales have more specialized crania and all come from marine sediments. Cetacea are classified in three suborders: Archaeoceti for archaic Eocene whales including *Basilosaurus*, Odontoceti for Oligocene-to-Recent toothed whales, and Mysticeti for Oligocene-to-Recent baleen whales (3).
2. P. D. Gingerich *et al.*, *Science* **220**, 403 (1983).
3. L. G. Barnes, D. P. Domning, C. E. Ray, *Mar. Mammal Sci.* **1**, 17 (1985).
4. J. Struthers, *J. Anat.* **15**, 141 (1881); *ibid.* (new series), **7**, 291 (1893); O. Abel, *Denkschr. Kaiserl. Akad. Wiss. Vienna Math.-Naturwiss. Kl.* **81**, 139 (1908); E. Lonnberg, *Ark. Zool.* **7** (no. 10), 1 (1910); D. A. Parry, *Proc. Zool. Soc. London* **119**, 51 (1949).
5. W. M. A. de Smet, *Z. Säugetierkd.* **40**, 299 (1975).
6. G. Guldberg, *Anat. Anz.* **9**, 92 (1894); H. C. Müller, *Arch. Naturgesch.* **7**, 1 (1920); T. Ogawa, *Sci. Rep. Whales Res. Inst.* **8**, 127 (1953).
7. R. C. Andrews, *Am. Mus. Novit.* **9**, 1 (1921); T. Ogawa and T. Kamiva, *Sci. Rep. Whales Res. Inst.* **12**, 197 (1957); T. Nemoto, *ibid.* **17**, 79 (1963); S. Ohsumi, *ibid.* **19**, 135 (1965). The rudimentary limb described by Andrews was said to include a femur, tibia, tarsus, and metatarsus; only two were ossified, and these are best interpreted as a femur and tibia with intervening connective cartilage. Tar-

- sal and metatarsal bones are not found in extant whales.
8. R. Harlan, *Trans. Am. Philos. Soc. (new series)*, **4**, 397 (1834). See Kellogg (14) for full history.
  9. R. Owen, *Trans. Geol. Soc. London Ser. 2*, **6**, 69 (1839). Owen's genus *Zeuglodon* is a junior synonym of *Basilosaurus*.
  10. *Basilosaurus cetoides* was named by Owen (9); its age is late Jacksonian (14), correlated with Priabonian late Eocene by W. G. Siesser *et al.* [*Geol. Soc. Am. Bull.* **96**, 827 (1985)]. *Basilosaurus isis* was named by H. J. L. Beadnell [in C. W. Andrews, *Geol. Mag. London Ser. 5*, **1**, 214 (1904)]; its age is middle Mokattamian, correlated with Bartonian late middle Eocene (17). *Basilosaurus isis* probably lived from about 42 to 40 million years before present.
  11. L. G. Barnes and E. Mitchell, in *Evolution of African Mammals* [V. J. Maglio and H. B. S. Cooke, Eds. (Harvard Univ. Press, Cambridge, MA, 1978), pp. 582-602], provide the most recent review of Egyptian archaeocetes. They follow Kellogg (14) and place *B. isis* in *Prozeuglodon*.
  12. F. A. Lucas, *Proc. U.S. Nat. Mus.* **23**, 327 (1900).
  13. J. W. Gidley, *ibid.* **44**, 649 (1913).
  14. R. Kellogg, *A Review of the Archaeoceti* (Carnegie Institution of Washington, Washington, DC, 1936).
  15. These smaller archaeocetes include specimens of *Prozeuglodon atrox* described by C. W. Andrews [*A Descriptive Catalogue of the Tertiary Vertebrata of the Fayum, Egypt* (British Museum, London, 1906)]. The holotype of *P. atrox*, type species of *Prozeuglodon*, is an immature skull from Zeuglodon Valley, where immature skulls this size associated with dorudontine vertebral columns are common, and immature skulls associated with basilosaurine vertebral columns are unknown. Thus *Prozeuglodon* is almost certainly dorudontine and not basilosaurine, *P. atrox* is not a synonym of *B. isis*, and *Prozeuglodon* is not available as a distinct genus for what is here called *B. isis* [compare (11) and (14)]; see also Fig. 2].
  16. H. J. L. Beadnell, *The Topography and Geology of the Fayum Province* (Survey Department, Cairo, 1905).
  17. R. Said, *The Geology of Egypt* (Elsevier, Amsterdam, 1962); A. Strougo and M. A. Y. Haggag, *Neues Jahrb. Geol. Palaeontol. Monatsh.* **1984**, 46 (1984); A. Strougo and M. A. Boukhary, *Revue Micropaléontol.* **30**, 122 (1987).
  18. In previous descriptions of USNM 12261, *B. cetoides*, Lucas (12) interpreted the pubic symphysis of each innominate as its posterior end. Gidley (13) and Kellogg (14) accepted this, but reversed left and right innominates. Some question remains as to which innominate is left and which is right; reversing these would have little effect on the reconstruction discussed here. Gidley confused proximal and distal ends of the partial femur, and Kellogg reversed the head and greater trochanter (most of the head is missing). In the meantime, Abel (19) interpreted the innominates as coracoids of a new Eocene bird, *Alabamomis gigantea*, and Stromer (20) compared them to innominates of the African water shrew *Potamogale*, and fancifully reconstructed ilia more than doubling their length. Innominate of *B. cetoides* are similar in length to those of *B. isis* but differ in being much broader anteroposteriorly. The partial femur of *B. cetoides* differs in having a much narrower greater trochanter.
  19. O. Abel, *Centralbl. Mineral. Geol. Palaeontol.* **1906**, 456 (1906).
  20. E. Stromer, *Sitzb. Bayer. Akad. Wiss. München Math.-Phys. Kl.* **1921**, 54 (1921).
  21. A. Boyden and D. Gemeroy, *Zoologica* **35**, 145 (1950).
  22. L. Van Valen, *Am. Mus. Nat. Hist. Bull.* **132**, 90 (1966).
  23. A. S. Romer, *Vertebrate Paleontology* (Univ. of Chicago Press, Chicago, 1966).
  24. We collected the proximal half of a femur and a complete patella associated with a dorudontine skeleton (ZV-72) in Zeuglodon Valley in 1989 before these elements were found with *B. isis* and before they could be positively identified. Given what we now know, these fossils show that one small archaeocete had hind limbs, but their full size, form, and possible function cannot be determined until they are better known.

25. We thank the Egyptian Geological Survey and Mining Authority and Mme. Ferial El Bedewi, director of the Cairo Geological Museum, for support of field work. A. A. Barakat, A. A. Abd Ellatif, and W. J. Sanders helped in the field and Y. Attia and P. Chatrath provided logistical support. We thank D. C. Fisher for help in interpreting the locking knee, and P. Webb for information on swimming in anguilliform vertebrates. We thank F. Ankel-Simons, L. G. Barnes, D. L. Domning, D. C. Fisher,

C. Gans, P. Myers, C. Ray, G. R. Smith, and F. C. Whitmore for reading the manuscript. Specimens were prepared by W. J. Sanders and illustrated by B. Miljour. Field research in Egypt in 1987 and 1989 was supported by the Duke University Fayum Expedition and by the National Geographic Society Committee on Research and Exploration (grants 3424-86 and 4154-89).

11 January 1990; accepted 25 April 1990

## Solution Structure of the Glucocorticoid Receptor DNA-Binding Domain

TORLEIF HÄRD,\* EDWIN KELLENBACH, ROLF BOELENES, BONNIE A. MALER, KARIN DAHLMAN, LEONARD P. FREEDMAN,† JAN CARLSTEDT-DUKE, KEITH R. YAMAMOTO, JAN-ÅKE GUSTAFSSON, ROBERT KAPTEIN‡

The three-dimensional structure of the DNA-binding domain (DBD) of the glucocorticoid receptor has been determined by nuclear magnetic resonance spectroscopy and distance geometry. The structure of a 71-residue protein fragment containing two "zinc finger" domains is based on a large set of proton-proton distances derived from nuclear Overhauser enhancement spectra, hydrogen bonds in previously identified secondary structure elements, and coordination of two zinc atoms by conserved cysteine residues. The DBD is found to consist of a globular body from which the finger regions extend. A model of the dimeric complex between the DBD and the glucocorticoid response element is proposed. The model is consistent with previous results indicating that specific amino acid residues of the DBD are involved in protein-DNA and protein-protein interactions.

THE GLUCOCORTICOID RECEPTOR belongs to a family of ligand-inducible nuclear transcription factors that include the steroid hormone, thyroid hormone, retinoic acid, and vitamin D<sub>3</sub> receptors. All members of this superfamily contain a highly conserved DNA-binding domain that consists of about 70 residues and mediates specific binding to hormone response elements on DNA (1). Protein fragments containing the glucocorticoid receptor DBD expressed in *Escherichia coli* exhibit sequence-specific binding to glucocorticoid response elements (GREs) (2, 3). These protein fragments contain two zinc atoms, tetrahedrally coordinated by conserved cysteine

residues, that are required for proper folding and DNA binding (2). The presence of zinc-binding domains is reminiscent of the "zinc finger" motif found in *Xenopus* TFIIIA (4), as well as similar domains found in retroviral nucleic acid binding proteins (5). However, the hormone receptor zinc-coordinating regions are not homologous to these other zinc fingers, suggesting that the DNA-binding domain of the steroid and thyroid hormone receptors constitutes a distinctive structural motif (6).

We have studied two protein fragments containing the glucocorticoid receptor DBD using two-dimensional nuclear magnetic resonance (2D NMR) and distance geometry (DG). These fragments contain 93 and 115 residues, respectively, with a

T. Härd, E. Kellenbach, R. Boelens, R. Kaptein, Department of Chemistry, University of Utrecht, Padualaan 8, 3584 CH Utrecht, The Netherlands.

B. A. Maler, L. P. Freedman, K. R. Yamamoto, Department of Biochemistry and Biophysics, University of California at San Francisco, San Francisco, CA 94143-0448.

K. Dahlman, J. Carlstedt-Duke, J.-Å. Gustafsson, Department of Medical Nutrition and Center for Biotechnology, Karolinska Institute, Huddinge University Hospital, S-141 86 Huddinge, Sweden.

\*On leave from Department of Medical Biophysics, Karolinska Institute, S-104 01 Stockholm, Sweden.

†Present address: Cell Biology and Genetics Program, Memorial Sloan-Kettering Cancer Center, New York, NY 10021.

‡To whom correspondence should be addressed.

**Fig. 1.** The segment Cys<sup>440</sup> to Arg<sup>510</sup> of the rat glucocorticoid receptor DNA-binding domain (Cys<sup>421</sup> to Arg<sup>491</sup> of the human glucocorticoid receptor) for which the three-dimensional structure is presented here (8). The boxed residues indicate amino acids that are essential for discrimination between glucocorticoid and oestrogen response elements (GRE and ERE) (26). The circled residues indicate the segment that is important for protein-protein interactions in the dimeric DBD-GRE complex (25).

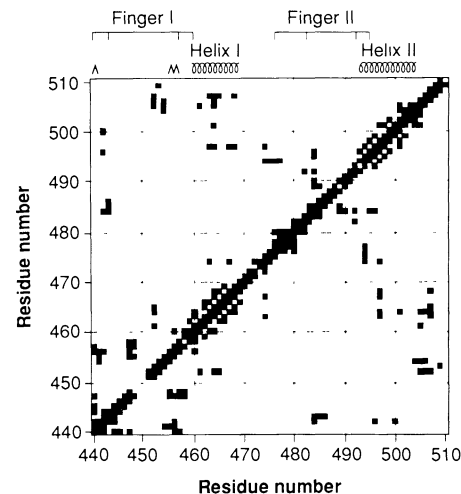
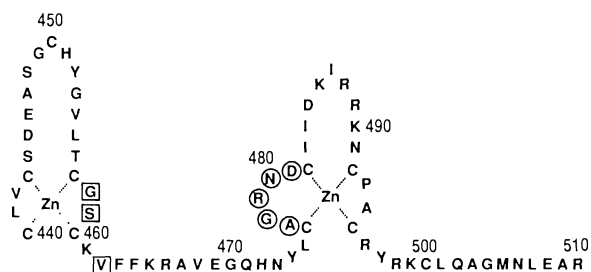


**Fig. 2.** Diagonal plot indicating residues between which NOEs have been found. Secondary structure elements and zinc coordination within the two finger domains (19) has also been indicated.

common sequence encompassing the Cys<sup>440</sup> to Ile<sup>519</sup> and Cys<sup>421</sup> to Ile<sup>500</sup> segments of the rat and human glucocorticoid receptors, respectively (7, 8). The structural studies focus on the 71-residue segment Cys<sup>440</sup> to Arg<sup>510</sup>, which includes the two zinc-coordinating finger regions (Fig. 1). Sequence-specific assignments of more than 90% of all observable <sup>1</sup>H resonances within this segment were obtained with the use of 2D double quantum filtered correlated spectroscopy (DQF-COSY), homonuclear Hartmann-Hahn spectroscopy (HOHAHA), and nuclear Overhauser enhancement spectroscopy (NOESY). The resonance assignments (9) were carried out with the use of well-established procedures (10, 11).

Several elements of secondary structure within the Cys<sup>440</sup> to Arg<sup>510</sup> segment could be identified based on characteristic patterns of NOE connectivities (10). These elements include two  $\alpha$ -helical regions encompassing Ser<sup>459</sup> to Glu<sup>469</sup> and Pro<sup>493</sup> to Gly<sup>504</sup>, a type I reverse turn between residues Arg<sup>479</sup> to Cys<sup>482</sup>, a type II reverse turn between residues Leu<sup>475</sup> to Gly<sup>478</sup>, a short stretch of antiparallel  $\beta$  sheet involving residues Cys<sup>440</sup> and Leu<sup>441</sup> and Leu<sup>455</sup> to Cys<sup>457</sup>, as well as